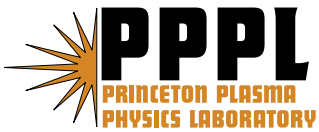

Princeton Plasma Physics Laboratory

PPPL-

PPPL-



Prepared for the U.S. Department of Energy under Contract DE-AC02-76CH03073.

Princeton Plasma Physics Laboratory

Report Disclaimers

Full Legal Disclaimer

This report was prepared as an account of work sponsored by an agency of the United States Government. Neither the United States Government nor any agency thereof, nor any of their employees, nor any of their contractors, subcontractors or their employees, makes any warranty, express or implied, or assumes any legal liability or responsibility for the accuracy, completeness, or any third party's use or the results of such use of any information, apparatus, product, or process disclosed, or represents that its use would not infringe privately owned rights. Reference herein to any specific commercial product, process, or service by trade name, trademark, manufacturer, or otherwise, does not necessarily constitute or imply its endorsement, recommendation, or favoring by the United States Government or any agency thereof or its contractors or subcontractors. The views and opinions of authors expressed herein do not necessarily state or reflect those of the United States Government or any agency thereof.

Trademark Disclaimer

Reference herein to any specific commercial product, process, or service by trade name, trademark, manufacturer, or otherwise, does not necessarily constitute or imply its endorsement, recommendation, or favoring by the United States Government or any agency thereof or its contractors or subcontractors.

PPPL Report Availability

Princeton Plasma Physics Laboratory:

<http://www.pppl.gov/techreports.cfm>

Office of Scientific and Technical Information (OSTI):

<http://www.osti.gov/bridge>

Related Links:

[U.S. Department of Energy](#)

[Office of Scientific and Technical Information](#)

[Fusion Links](#)

Fast Soft X-ray Images of MHD Phenomena in NSTX*

C.E. Bush¹, B.C. Stratton², J. Robinson², L.E. Zakharov², E. D. Fredrickson², D. Stutman³, K. Tritz³

¹Oak Ridge National Laboratory, Oak Ridge, TN bush@pppl.gov

²Princeton Plasma Physics Laboratory, Princeton, NJ bstratton@pppl.gov

³Johns Hopkins University, Baltimore, Md ktritz@pppl.gov

ABSTRACT

A variety of MHD phenomena have been observed on NSTX. Many of these affect fast particle losses, which are of major concern for future burning plasma experiments. Usual diagnostics for studying these phenomena are arrays of Mirnov coils for magnetic oscillations and PIN diode arrays for soft x-ray emission from the plasma core. Data reported here are from a unique fast soft x-ray imaging camera (FSXIC) with a wide-angle (pinhole) tangential view of the entire plasma minor cross section. The camera provides a 64x64 pixel image, on a CCD chip, of light resulting from conversion of soft x-rays incident on a phosphor to the visible. We have acquired plasma images at frame rates of 1-500 kHz (300 frames/shot), and have observed a variety of MHD phenomena: disruptions, sawteeth, fishbones, tearing modes, and ELMs. New data including modes with frequency > 90 kHz are also presented. Data analysis and modeling techniques used to interpret the FSXIC data are described and compared, and FSXIC results are compared to Mirnov and PIN diode array results.

I. INTRODUCTION

The Fast Soft X-ray imaging camera is now established as a major diagnostic for study of magnetohydrodynamic (MHD) instabilities in high temperature magnetically confined plasmas. It has

* Contributed paper, published as part of the Proceedings of the 17th Topical Conference on High-Temperature Plasma Diagnostics, Albuquerque, New Mexico, May 2008.

now been used for MHD studies on several toroidal fusion research devices. These include the Tokamak Experiment for Technology Oriented Research (TEXTOR), the Large Helical Device (LHD), and the National Spherical Torus Experiment (NSTX) at the Princeton Plasma Physics Laboratory. Theory indicates that the alpha heating power in sawtoothing ITER discharges could be reduced compared to non-sawtoothing plasmas. Effects on alphas have been observed experimentally during sawtoothing DT discharges on TFTR and JET. Theory and experiment also indicate that sawteeth cause redistribution of fast particles resulting from NBI. It is important for STs, ITER, and ITPA database aspect ratio scaling to understand the spatial structure of the associated modes in order to understand how they interact with the fast particles. We have studied the spatial structure and time behavior of the MHD in NSTX using Fast Soft X-ray Camera Imaging. This includes use of a range of Be foil thicknesses to investigate different parts of the soft X-ray spectra emitted from the high temperature NSTX plasma, much of which may be associated with different MHD modes. Highly reproducible and strongly sawtoothing target plasmas are also used. One example was a 1 second duration discharge, which showed EPMs early in the shot and later, sawteeth, when the q was reduced. In addition it is possible the sawteeth could trigger NTMs. The target discharges include L-mode, H-mode, and He plasmas.

The goal is to study the physics of the interaction of the MHD with the plasma on NSTX using fast soft x-ray camera imaging. We have acquired plasma images at frame rates of 1-500 kHz, and have observed a variety of MHD phenomena: internal reconnection events, disruptions, sawteeth, fishbones, tearing modes, and ELMs. This is important to ITER due to fast particle (α 's, etc.) losses.

II. EXPERIMENTAL SETUP

The pinhole camera with a wide-angle tangential view of the plasma [1-4] is based on the Princeton Scientific Instruments PSI-5 CCD camera. It has a 64 X 64 pixel image, and frame rates up to

500 kHz for 300 frames. The soft x-rays ($\sim 1-5$ keV) are converted to visible light by fast P47 phosphor deposited on a fiber-optic faceplate, and an electrostatic image intensifier and lenses de-magnify the image by 6:1 and couple visible light to the CCD. The size (1-5 mm diameter) of the pinhole can be changed from a remote location (remotely selectable), in the case of NSTX, the control room. This allows tradeoff of spatial resolution and signal level, and the remotely selectable beryllium foils allow low-energy cutoff of the soft X-rays incident on the phosphor to be varied. The horizontal field-of-view of the fast soft x-ray imaging camera (FSXIC) includes nearly the full minor cross-section of the NSTX chamber.

In NSTX, β_t is normally relatively high such that the hot core is Shafranov shifted toward the low B_t field side of the cross section that is always fully viewed by the FSXIC. This cross section is viewed through a pinhole, which is essentially the entrance of the X-rays to the camera system. Behind the pinhole is the filter array, which includes the remotely selectable array of foils of various thicknesses and materials (Be, Ti). This variety of filters and apertures allow viewing of a wide spectrum of plasma temperatures and MHD behavior. Much of the data to date have been obtained using the thinner Be foils, mainly a 7.6 mm Be foil, thus limiting observation to lower temperature (often ohmic) plasmas. In many cases coherent modes and their time behavior and spatial extent are clearly discernable in the images before additional processing.

III. RESULTS AND DISCUSSION

A good example illustrating the effectiveness of images (or snapshots) of MHD activity is that of discharge (shot) 113778). Two images, beginning at $t = 0.176$ s, of the recorded 300 frames (images) taken are shown in Figure 1. In each image, low intensity is represented by dark shades or colors and high intensity by light colors to a maximum represented by white. The two images are representative of the extremes of the first half of each cycle of the mode. A half cycle begins with Fig 1(a) and ends with

Fig 1(b), in both of which the highest intensity region is centered about the midplane. A movie of the 300 images shows the high intensity spot to begin shifting downward. This continues for a few frames, then the high intensity spot shifts to the right, and then upward until it again reaches the midplane where it has acquired the shape of the image in Fig 1(b). Then for the 2nd half, the high intensity spot shifts upward, to the left and down as it progresses back to Fig 1(a). Thus the train of 300 frames i.e. 64x64 pixel image/snapshot shows the time evolution of the mode structure.

In this case the dynamics of the images correlated very well with data from core chordal data of an array of soft X-ray (SXR) diodes. Figure 2 shows time traces for a centrally viewing and two off axis viewing SXR diodes. The SXR diodes show the mode to turn on at $t = 0.1735$ s, and oscillate at 2.5 kHz through the time of Fig. 2. The camera was run at 100 kHz (10 μ s/frame) for 3 ms beginning at $t = 0.175$ s, missing the first 2 or 3 cycles, and ending at $t = 0.178$ s.

The $m/n=1/1$ tearing mode of Fig 2 was observed using the FSXIC images, which showed structure with coherent oscillations. This was in agreement with the (central) chords of the SXR array data plotted in Fig.2. The plasma current was $I_p = 500$ kA. The effects of the mode were seen in the stored energy, which decreased rapidly at the onset of the mode at $t = 0.174$ s. A Singular value decomposition (SVD) analysis was done of the full train of images [5], 300 frames, from $t = 0.175$ s to $t = 0.178$ s. The SVD was used in order to extract separate coherent fluctuations in space and time from background noise. SVD analysis identifies major components of the dynamics recorded in the images. The camera images yield a matrix $A(M \times N)$ of N time series of M frames, where $M = 300$ frames per shot. The matrix A is decomposed into 3 matrices such that

$$A(M \times N) = U W V^T.$$

Where:

$U (M \times N)$ - columns are spatial vectors (topos)

$V(N \times N)$ - columns are temporal vectors (chronos) and $W(N \times N)$ - a diagonal matrix (of weights)

Figure 3 summarizes results of the SVD, Figure 3a and b-f and g-k, where b-f are the time (chronos, $V_0 - V_4$) behaviors of the first five dominant modes and g-k are the respective spatial structures (topos, $U_0 - U_4$) for each of the chronos. Note that the oscillations in 3d and 3e match up exactly with the same time of the oscillations in the SXR diode traces of Fig 2

Figure 4 shows two frames of a second plasma that were taken 2 ms apart. A centrally viewing (perpendicular) SXR diode trace for the plasma is shown in Figure 5. The MHD mode is triggered at $t = 0.226$ s, beginning at a modest oscillation frequency and slows to a lower frequency toward the end of the burst. In this case the FSXIC was operated at 10 kHz, so that the 300 frames covered 30 ms, or nearly the full duration of the MHD burst. Again a SVD analysis of the images was done and the results are shown in Figure 6 (shot 113355). The chronos, V_3 and V_4 , extracted by the SVD clearly match the SXR diode time trace of Fig. 5. Some of the major topos are slightly more complex in this case than those for the case of Fig, 3.

Results for a third and final example are given in Figures 7 and 8. The main difference for this case was that the camera was run at 500 kHz and therefore was able to capture higher frequency MHD phenomena. In this case the 300 frames were acquired at $2 \mu\text{s}/\text{frame}$ for 0.6 ms of the discharge beginning at 0.2500 s and ending at 0.2506 s. The oscillations were very clear and detailed in the movie of the 300 images, beginning with a quiescent frame to frame behavior then showing triggering of a mode having a high frequency, growing in amplitude while gradually slowing, peaking and then slowly decreasing in amplitude and disappearing, all during the 300 frames (0.6 ms). This Activity is shown quantitatively in the SVD results given in Fig.7. A main difference in SVD results for the third example from the first two is that no coherent modes were found in the first 5 chronos, but only in the second

five, V7 and V8 respectively . From the SVD it was determined that the mode frequency was ~ 90 kHz, and this result is to be compared to the magnetics data described in the next paragraph.

Figure 8 shows results from analysis of data from Mirnov coil arrays, and is a plot of the spectra of magnetic fluctuations versus time. The FSXIC data was taken within 0.6 ms of the beginning of the plot at 0.25 s. The frequency data is plotted from 0.25 to 0.30 s. The Mirnov data shows coherent activity at 3 MHD mode values, $n=2, 3,$ and 4 at $70, 90,$ and 110 kHz respectively during the first 10 ms of the plot. The $n=3$ mode agrees with the 90 kHz mode given by the SVD analysis of the train of FSXIC images.

A code (Cbbst) [6] was written to simulate the line integral of the camera data and to invert it assuming a simple spatial dependence of $\epsilon = \epsilon(a + \xi)$, where a is a flux surface label corresponding to the square root of the toroidal magnetic flux and $\xi(a, \theta, \varphi)$ is a perturbation that may include both ideal and tearing types of perturbations. Step-like $m/n=1/1$ perturbations were considered. For this report a simulation was done for the example plasma of Figs 4-6, however the technique is also applicable to the other two plasma examples. The results of the simulation are given in Figure 9.

The 21 radial values of the $\epsilon(a_i)$ function and the amplitude and phase of the $\xi_{1/1}$ perturbation are reconstructed from the 64×64 data array S_{ij} using singular value decomposition and an iterative technique for solving the integral equation, which becomes non-linear in the presence of perturbations. The plasma equilibrium was generated by the Equilibrium and Stability Code [4] using a plasma boundary reconstructed by the EFIT code and TRANSP code simulations of plasma pressure and q profiles. It is clear that the results of the simulation, Figs 9 (c) and (d) agree well with the surface, 9(a), and contour, 9(b), plots of the experimental FSXIC data.

IV. CONCLUSIONS

A variety of MHD cases have been investigated on NSTX using the FSXIC. Three cases were presented and discussed in this report. Possible existence of MHD modes was indicated simply by viewing movies made from FSXIC images. Simple $m/n=1/1$ modes were clear in the camera images and in results of SVD analysis. An $n=3$ mode determined from the combination of SVD analysis of FSXIC images and magnetic fluctuation data was shown. Results for operation of the camera at three framing rates, 10, 100, and 500 kHz showed MHD modes at frequencies from a low of 2 kHz to a high of 90 kHz. SVD analysis was effective in determining mode frequencies and spatial structure. These were found to agree with or compliment results from SXR array and Mirnov coil array data.

ACKNOWLEDGMENTS

The authors would like to give special thanks to Doug Labrie of the NSTX team of PPPL and Vince Mastrocola of Princeton Scientific Instruments. We also thank Dr. Satoshi Ohdachi for providing the software for carrying out the SVD analyses. This work was supported in part by US DOE contracts DE-AC05-00OR22725 and DE-AC02-76CH03073.

REFERENCES

1. S. von Goeler, *et al.*, Rev. Sci Instrum. **70** (1999) 599.
2. B. C. Stratton, *et al.*, Rev. Sci Instrum. **75** (2004) 3959.
3. B.C. Stratton, S. von Goeler, D. Stutman, K. Tritz, and L.E. Zakharov, “*Be Foil Filter Knee Imaging NSTX Plasma with Fast Soft X-Ray Camera*”, 32nd EPS Conference on Plasma Phys. Tarragona, 27 June - 1 July 2005 ECA Vol.**29C**, P-1.060 (2005)

4. B.C. Stratton, S. von Goeler, D. Stutman, K. Tritz, and L.E. Zakharov, “*Be Foil Filter Knee Imaging NSTX Plasma with Fast Soft X-Ray Camera*”, PPPL Report PPPL-4093, August 2005
5. S. Ohdachi *et al.* Rev. Sci. Instrum., **74 (2003)** 2136.
6. L. E. Zakharov and A. Pletzer, Phys. Plasmas **6** (1999) 4693

Figure Captions

Fig. 1. FSXIC images for two frames of the 300 recorded for shot 113778.

Fig. 2. I_p , and three SXR diode time traces for shot 113778. The first is for a centrally viewing diode and the second is for a diode viewing below and the third for a diode viewing above the midplane.

Fig. 3. Results of SVD for shot 113778.

Fig. 4. Two consecutive (in time) FSXIC frames for shot 113355.

Fig. 5. SXR diode trace for shot 113355.

Fig. 6. SVD for shot 113355. The chronos match the time behavior of the SXR diode of Fig. 5.

Fig. 7. SVD for a shot (124771) for which the FSXIC showed a high frequency, 90 kHz, $n=3$ MHD mode.

Fig. 8. Time resolved spectra of magnetic fluctuations from arrays of Mirnov coils. Clearly indicated is the existence of $n=3$ fluctuations at 90 kHz at the same time of the modes with the same frequency indicated in the SVD analysis of Fig 7.

Fig. 9. (a) Surface and (b) contour plots of actual plasma emissivity (from FSXIC images) for shot 113355. The reconstructions are shown in (c) and (d) respectively.

Figure 1

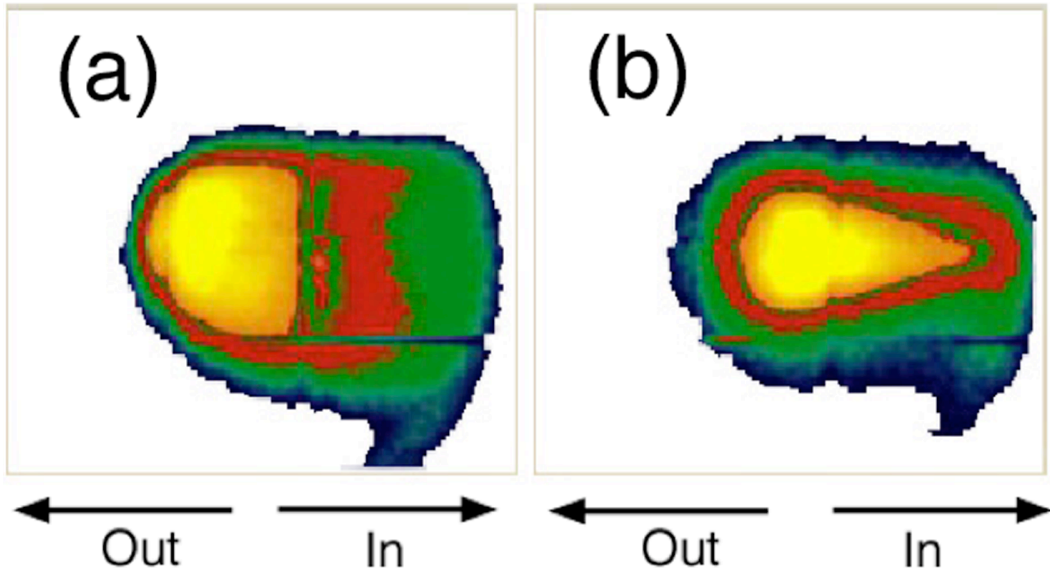


Figure 2

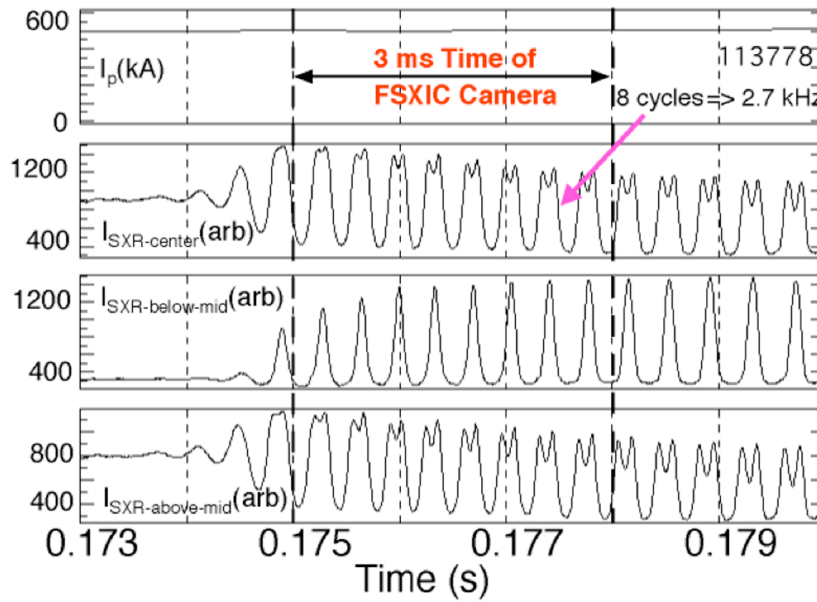


Figure 3

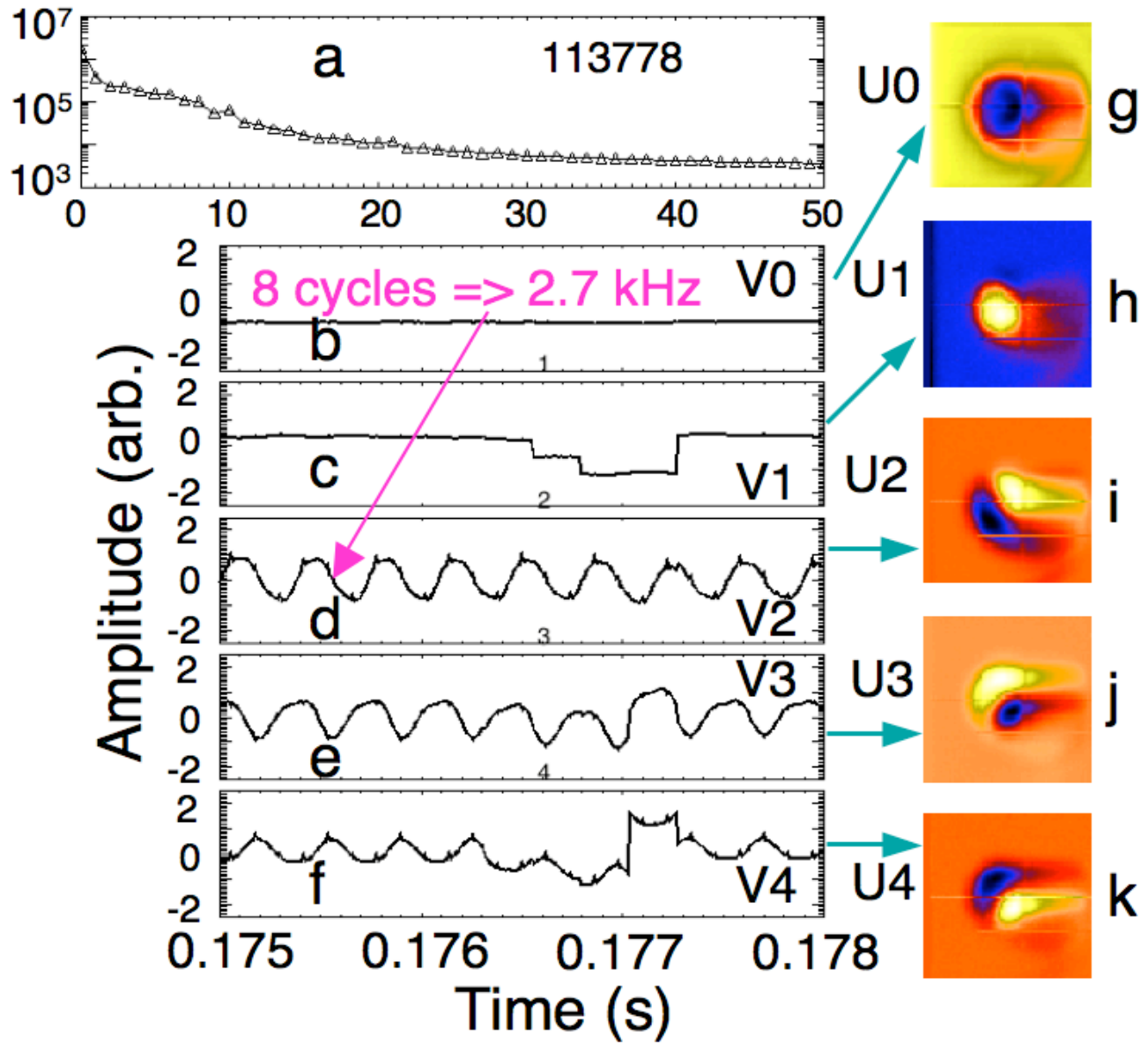


Figure 4

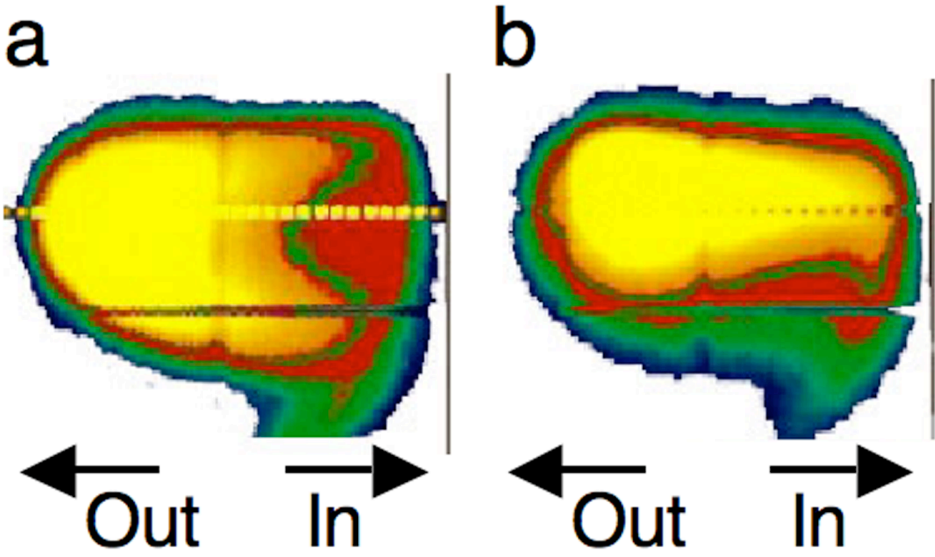


Figure 5

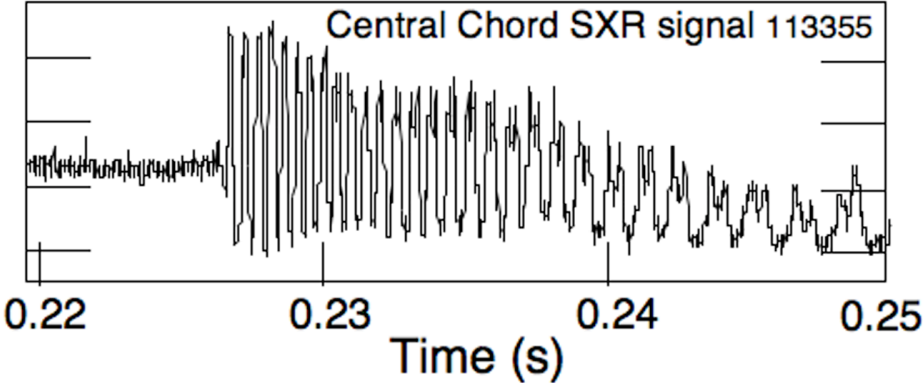


Figure 6

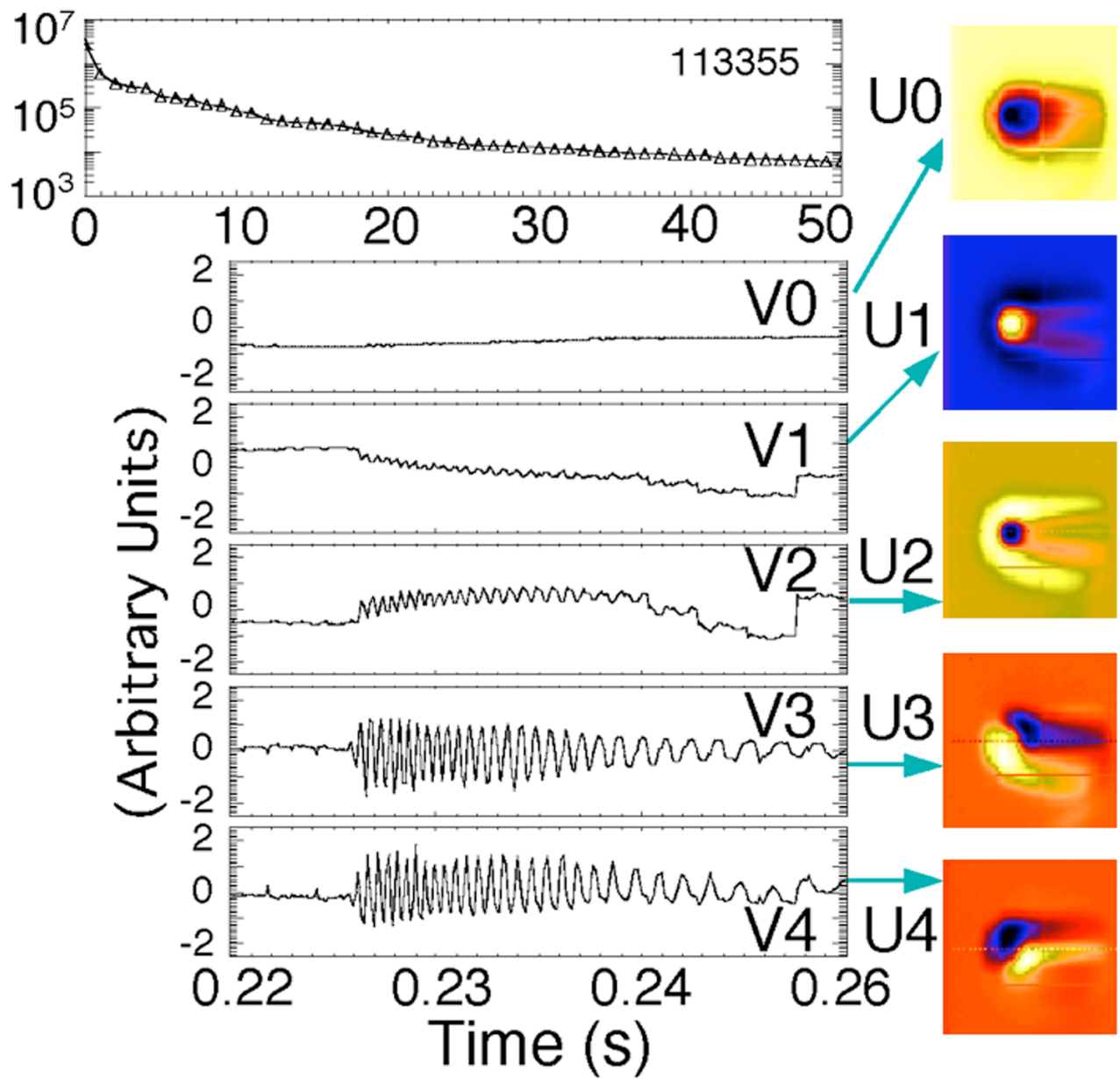


Figure 7

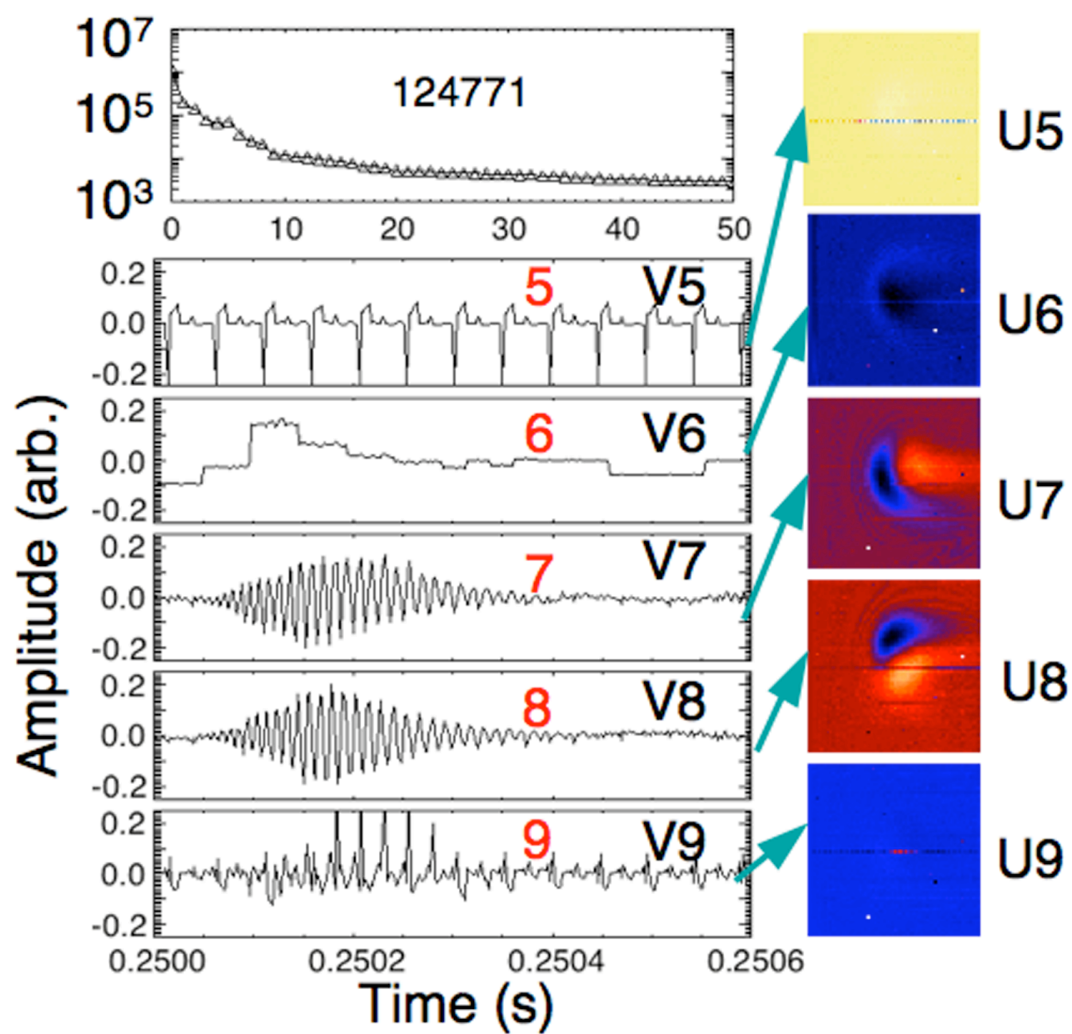


Figure 8

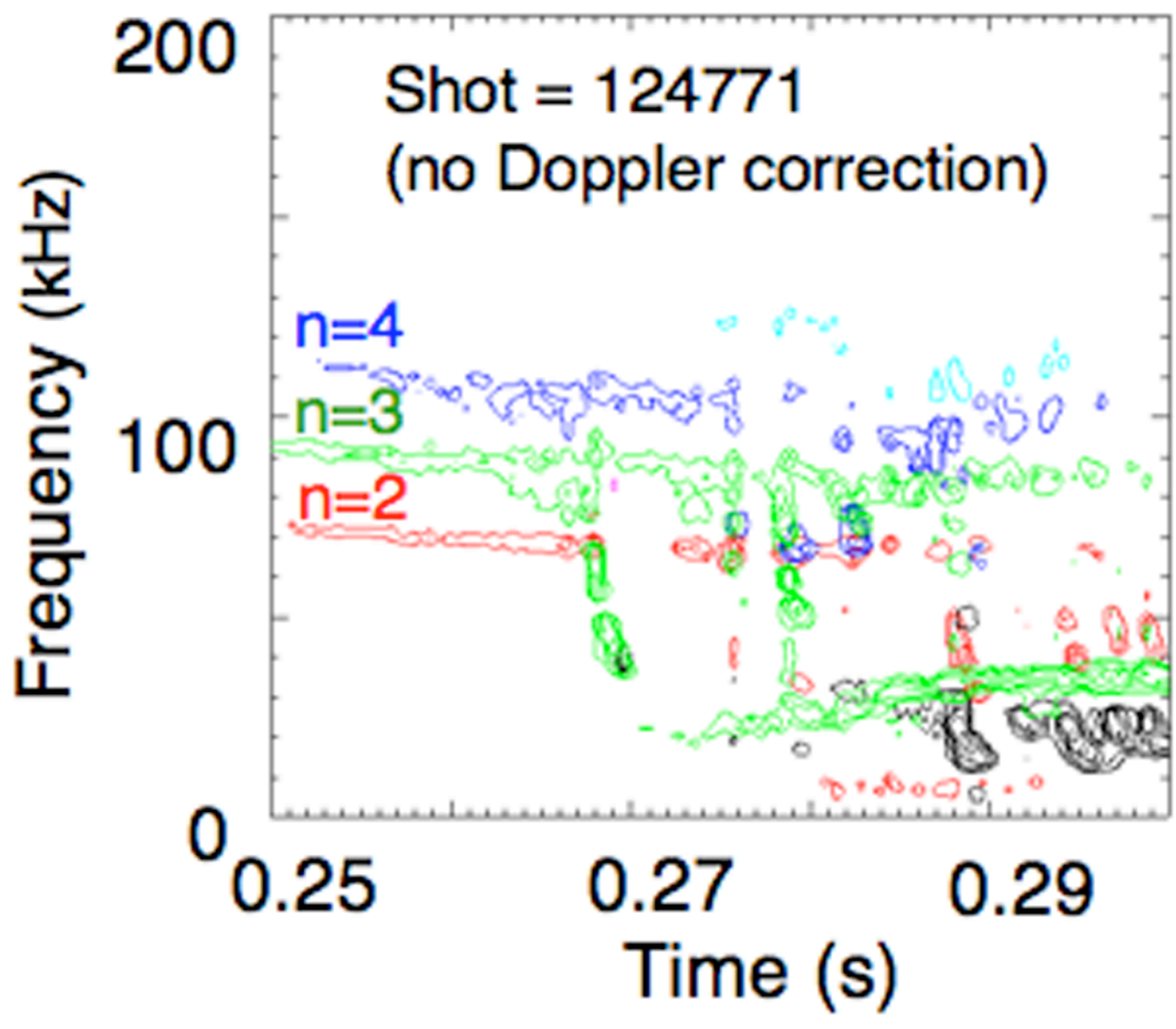
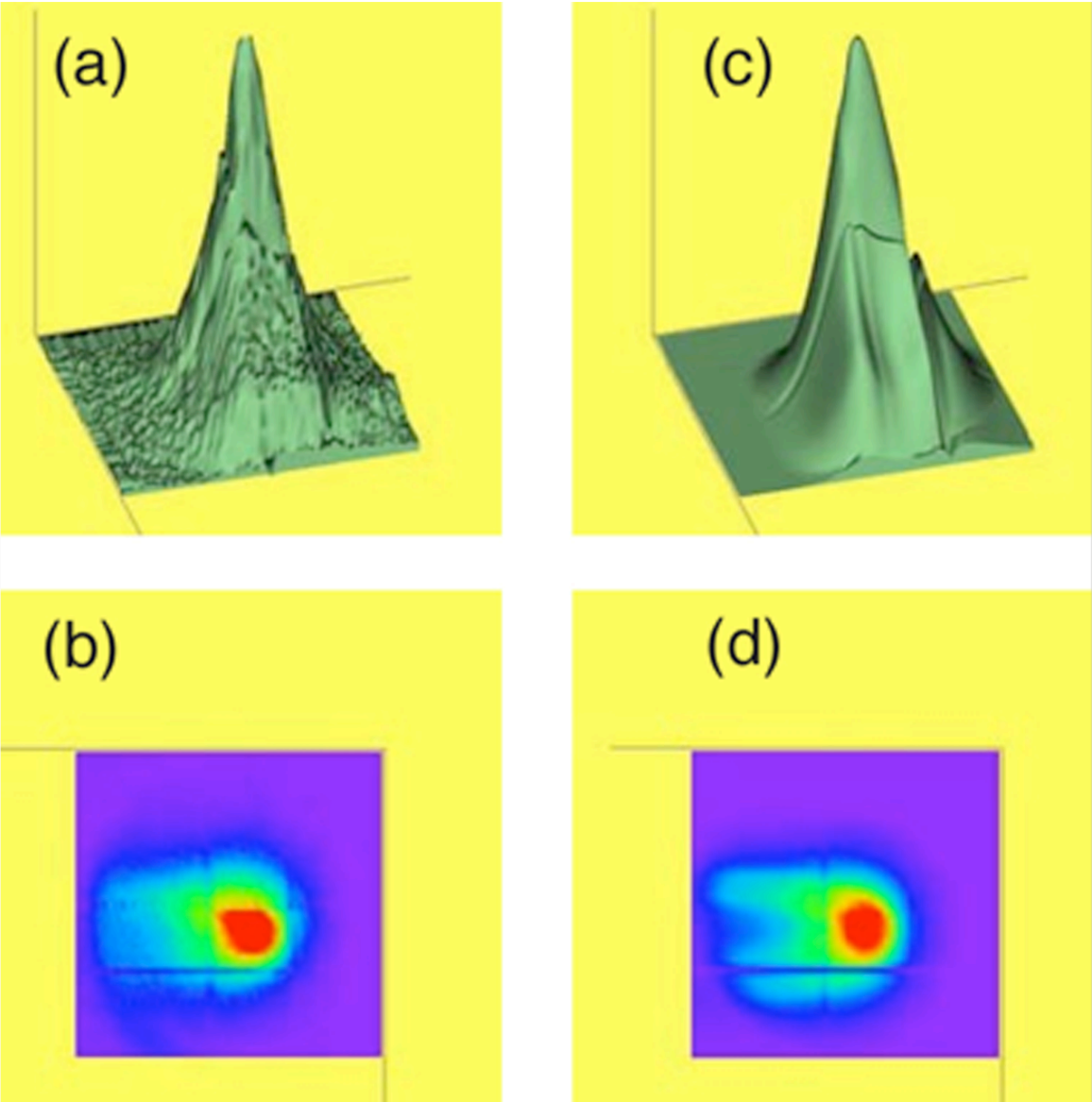


Figure 9



The Princeton Plasma Physics Laboratory is operated
by Princeton University under contract
with the U.S. Department of Energy.

Information Services
Princeton Plasma Physics Laboratory
P.O. Box 451
Princeton, NJ 08543

Phone: 609-243-2750
Fax: 609-243-2751
e-mail: pppl_info@pppl.gov
Internet Address: <http://www.pppl.gov>